

**ALUMINUM, GALLIUM, INDIUM AND IRON SUPPORTED
ONTO RICE HUSK ASH SILICA AS CATALYSTS FOR
THE FRIEDEL-CRAFTS ALKYLATION REACTIONS
OF AROMATIC COMPOUNDS**

by

ADIL ELHAG AHMED MOHAMED SALIH

**Thesis submitted in fulfillment of the
requirements for the degree of
Doctor of Philosophy**

November 2008

ACKNOWLEDGEMENTS

I am pleased to place on record my gratitude and thanks to the government of Sudan, the government of Malaysia, Sudan University of Science and Technology and University Science Malaysia for the financial, academic and technical supports.

I really like to express my deep feeling of gratitude to my supervisor, Associate Professor Dr. Farook Adam for his patience, kindness, encouragement and good listening. I am very grateful to his unlimited guidance and continuous support through the research period. Without his help, this research would not progress smoothly.

I am also grateful to the technical staff, namely: Mr. Kanthasamy Subramaniam, Mr. Aw Yong, Mr. Yee, Mr. Nazeef, Mr. Ong Chin Hwie, Mr. Karuna, Mr. Muthu, Mr. Jauhar and Madam Jamilah for their nice help in the nitrogen adsorption analysis, GC/GC-MS, ICP-MS, XRD, electron microscopy analysis, respectively. My gratitude is also due to Ibnu sina centre (UTM, Malaysia), Combicat centre (UM, Malaysia), Indian Institute of Technology (IIT Madras) for their efforts to achieve the solid-state NMR and ESR analysis.

I would like to extend my sincere thanks to Mrs. Joo Hann for knowledge sharing and endless help. I also thank Mrs. Tan Hooi Hooi for her nice assistant regarding the GC-MS analysis. My thanks are also due to my colleagues Mr. Vejaykumaran, Mr. Naser Eltaher, Mrs. Ishragaa Abdulmoniem, Ms. Jeyashelly, Mr. Anwar Igbal, Ms. Mardiana Saied, Ms. Nurarisma, Mr. Kasim Almousawi and Dr. T. Radhika for their cooperation and helps in completing this work.

I always deeply indebted to my parents (Elhag Ahmed and Aamnah Mohamed) and my brothers and sisters who are continuously encouraging and supporting me in working towards higher degree in science. I'll never ever forget their spiritual support, continuous praying and making doaa to Allah for help. My acknowledgements are also go to my father, mother and sisters in law for their encouragement and spiritual support.

Finally, I wish to express my very warm sincere to my wife Maazza Yousuf and the two lovely kids Ahmed and Yousuf for always being by my side and supporting me all the way during the often busy and stressful times at Universiti Sains Malaysia.

TABLE OF CONTENTS

	Page
Acknowledgements.....	ii
Table of contents.....	iii
List of tables.....	ix
List of figures.....	xii
List of schemes.....	xv
List of symbols and abbreviations	xvi
List of appendices.....	xix
Abstrak.....	xxi
Abstract.....	xxii
	i
Chapter 1 – Introduction	
1. Introduction.....	
1.1 Silica.....	1
1.1.1 The occurrence of silica.....	3
1.1.2 Surface species of silica.....	3
1.1.3 Types and phases of silica.....	4
1.1.4 The sol-gel process.....	4
1.1.5 Activation and de-activation of silica surface.....	7
1.1.6 Structures of porous xerogels and aerogels.....	11
1.2 Friedel –Crafts reaction.....	12
1.2.1 Back ground.....	13

1.2.2	Orientation and reactivity.....	13
1.2.3	Catalysts.....	15
1.2.3.1	Homogeneous catalysts.....	18
1.2.3.2	Heterogeneous catalysts.....	18
1.2.4	Types of supporting materials.....	19
1.3	Rice husk.....	21
1.3.1	Composition and production.....	23
1.3.2	Production of silica from rice husk.....	23
1.3.3	Usages of RH, RHA and silica extracted from RHA.....	24
1.3.4	Modification of RHA silica for catalytic reactions.....	26
1.4	The objectives of the study.....	28
		29

Chapter 2 – Experimental Methods

2.1	Raw materials.....	
2.2	Extraction and modification of silica from RHA.....	31
2.2.1	Washing and treatment of RH.....	31
2.2.2	Preparation of silica.....	31
2.2.3	Preparation of the catalysts.....	32
2.3	Physico-chemical characterization.....	32
2.3.1	Fourier transform infra red spectroscopy.....	33
2.3.2	Nitrogen adsorption analysis.....	33
2.3.3	²⁹ Si MAS NMR spectroscopy.....	34
2.3.4	²⁷ Al and ⁷¹ Ga MAS NMR spectroscopy.....	34
2.3.5	Electron spin resonance (ESR).....	34
2.3.6	Powder X-ray diffraction (XRD).....	35

2.3.7	Scanning electron microscopy - Energy dispersive x-ray.....	35
2.3.8	Transmission electron microscopy (TEM).....	35
2.3.9	Inductively coupled plasma mass spectroscopy (ICP-MS).....	36
2.4	Catalytic reactions.....	36
2.4.1	Reaction procedures.....	37
2.4.2	Gas chromatography.....	37
		38

Chapter 3 – Characterization of the catalysts

3.1	Infrared spectroscopy.....	
3.2	Solid-state MAS NMR.....	40
3.2.1	²⁹ Si MAS NMR.....	43
3.2.2	²⁷ Al MAS NMR.....	43
3.2.3	⁷¹ Ga MAS NMR.....	46
3.2.4	Electron spin resonance (ESR).....	47
3.3	Nitrogen adsorption analysis.....	48
3.4	Powder X-ray diffraction.....	49
3.5	Electron micrographs.....	56
3.6	Elemental analysis.....	58
3.7	Conclusion	60
		62

Chapter 4 – Catalytic benzylation of aromatics

Introduction.....	
Benzylation of benzene	64
Catalytic study.....	72
Influence of reactants molar ratio.....	72

The effect of catalyst weight.....	73
Influence of reaction temperature.....	75
Influence of metal ions loading.....	76
Influence of catalyst type.....	78
Reaction over metal salt.....	80
Reaction kinetics.....	84
Influence of electron donating substituent.....	86
Reaction mechanism.....	88
Recyclability.....	90
The heterogeneous nature of the catalytic reaction.....	92
Benzylation of <i>o</i>-, <i>m</i>- and <i>p</i>-xylene.....	93
4.3.1 Catalytic study.....	95
4.3.2 Influence of reactants molar ratio	95
4.3.3 Influence of reaction temperature.....	97
4.3.4 Influence of metal ions loading	99
4.3.5 Benzylation over metal salt.....	101
4.3.6 Influence of catalyst type.....	103
4.3.7 Comparison with other aromatics.....	105
4.3.8 Effect of different isomers.....	107
4.3.9 Reusability.....	109
4.3.10 Leaching test.....	113
4.4 Benzylation of chlorobenzene.....	113
4.4.1 Catalytic study.....	114
4.4.2 Influence of reactants molar ratio	114
4.4.3 Influence of reaction temperature.....	116

4.4.4	Effect of metal ions loading.....	119
4.4.5	Benzylation over metal salt.....	122
4.4.6	Influence of catalyst type.....	125
4.4.7	Reaction kinetics.....	126
4.4.8	Recyclability.....	128
4.4.9	Leaching test.....	130
4.4.10	Conclusion	131
		132
 Chapter 5 – Catalytic <i>tert</i>-Butylation of aromatics		
5.1	Introduction.....	
5.2	Catalytic study.....	135
5.2.1	Influence of reactants molar ratio	139
5.2.2	Influence of reaction temperature.....	142
5.2.3	Influence of catalyst type.....	144
5.2.4	Influence of metal ions loading.....	146
5.2.5	Catalytic reaction over metal salts.....	148
5.2.6	Reaction kinetics.....	151
5.2.7	<i>tert</i> -Butylation of different aromatics.....	153
5.2.8	<i>tert</i> -Butylation of different xylene isomers.....	155
5.2.9	The heterogeneous nature of the catalytic reaction.....	158
5.2.10	Recyclability.....	160
5.2.11	Conclusion	161
		163
 Chapter 6 – Conclusion & Recommendations.....		
		165

References.....	
Appendices.....	169
List of publications.....	184
List of conferences.....	217
	218

LIST OF TABLES

	Page
Table 2.1 The GC and GC-MS conditions for the separation and identification of the alkylation reactions products	39
Table 3.1 The N ₂ adsorption analysis data for RHA silica prepared from different concentrations of sodium hydroxide	54
Table 3.2 The N ₂ adsorption analysis data for RHA silica and metal modified silica samples	55
Table 3.3 The elemental analysis data for RHA silica and metal modified silica samples	62
Table 4.1 The product distribution with varying RHA-Ga catalyst mass for the benzylation of benzene at 80 °C and Bz/BC ratio of 15:1	76
Table 4.2 The product distribution for the reaction between Bz and BC with a molar ratio of 15:1 and at different temperatures using RHA-Ga	77
Table 4.3 The product distribution for Bz benzylation at 80 °C and Bz/BC ratio of 15:1 over RHA catalysts with varying loading of Ga ³⁺ ions	79
Table 4.4 The product distribution for the benzylation of Bz at 80 °C and Bz/BC ratio of 15:1 over different catalysts	83
Table 4.5 The product distribution for the benzylation of Bz at 80 °C using Bz/BC molar ratio of 15:1 and RHA-Ga or gallium nitrate as a catalyst	85
Table 4.6 The kinetic parameters for benzene benzylation reaction over different catalysts	87
Table 4.7 Re-usability of RHA supported catalysts (0.1 g) for the benzylation of benzene at 80 °C using Bz/BC molar ratio of 15:1.	93
Table 4.8 Stability of RHA catalysts against leaching for the benzylation of Bz at 80 °C using Bz/BC molar ratio of 15:1	94
Table 4.9 The product distribution for a reaction between <i>p</i> -Xyl and BC with a molar ratio of 15:1 and at different temperatures using RHA-In catalyst	101

Table 4.10	The product distribution with varying indium loading for the <i>p</i> -Xyl benzylation reaction at 80 °C using <i>p</i> -Xyl/BC molar ratio of 15:1.	103
Table 4.11	The product distribution for the benzylation of <i>p</i> -Xyl at 80 °C using <i>p</i> -Xyl/BC molar ratio of 15:1 and RHA-In or indium nitrate as a catalyst	105
Table 4.12	The reactivity of RHA-Ga for the benzylation of different aromatics (AR) at 80 °C using AR/BC molar ratio of 15:1	109
Table 4.13	The product distribution for the catalytic benzylation reactions of different xylene isomers at 80 °C using Xyl/BC molar ratio of 15:1	111
Table 4.14	Re-usability of RHA supported catalysts for the benzylation of <i>p</i> -xylene at 80 °C using <i>p</i> -Xyl/BC molar ratio of 15:1	113
Table 4.15	Stability of RHA catalysts against leaching for the benzylation of <i>p</i> -Xyl at 80 °C using <i>p</i> -Xyl/BC molar ratio of 15:1	114
Table 4.16	The product distribution for the benzylation of chlorobenzene at 90 °C over RHA-In using various molar ratios of CB/BC	120
Table 4.17	The product distribution for the benzylation of CB with BC at different temp. using CB/BC ratio of 15:1 and RHA-In catalyst	121
Table 4.18	The product distribution for the benzylation of CB at 90 °C and CB/BC molar ratio of 15:1 over RHA catalysts with varying indium ions loading	124
Table 4.19	The reaction profile for the benzylation of chlorobenzene with BC at 90 °C using CB/BC molar ratio of 15:1 and RHA-In or indium nitrate catalyst	126
Table 4.20	The product distribution for the benzylation of chlorobenzene at 90 °C and CB/BC molar ratio of 15:1 using different catalysts	128
Table 4.21	The kinetic parameters for chlorobenzene benzylation reactions over different catalysts	130
Table 4.22	Re-usability of RHA catalysts for the benzylation of chlorobenzene at 90 °C using CB/BC molar ratio of 15:1	131
Table 4.23	Leaching effect for RHA supported metal ions at 90 °C and CB/BC molar ratio of 15:1	132
Table 5.1	The product distribution for the <i>tert</i> -butylation of benzene at 80 °C over RHA-In catalyst using various molar ratios of Bz/TBC.	143
Table 5.2	The product distribution for the <i>tert</i> -butylation of benzene at different temperatures over RHA catalysts using Bz/TBC molar	148

ratio of 15:1

Table 5.3	The product distribution for the <i>tert</i> -butylation of Bz with TBC at 80 °C over RHA catalysts with varying indium ions loading using Bz/TBC molar ratio of 15:1	151
Table 5.4	The product distribution for the <i>tert</i> -butylation of Bz with TBC at 80 °C over homogeneous or heterogeneous catalysts using Bz/TBC molar ratio of 15:1	153
Table 5.5	The kinetic parameters for the <i>tert</i> -butylation of benzene over different catalysts	154
Table 5.6	The product distribution for the <i>tert</i> -butylation of aromatics (AR) at 80 °C over RHA-Fe catalyst using AR/TBC molar ratio of 15:1	157
Table 5.7	The product distribution with varying xylene isomers for the <i>tert</i> -butylation reactions of xylene with TBC at 80 °C using Xyl/TBC molar ratio of 15:1 and RHA-Fe catalyst	160
Table 5.8	Stability of RHA catalysts against leaching for the <i>tert</i> -butylation of benzene at 80 °C using Bz/TBC molar ratio of 15:1	161
Table 5.9	Re-usability of RHA catalysts for the <i>tert</i> -butylation of benzene at 80 °C using Bz/TBC molar ratio of 15:1	162

LIST OF FIGURES

		Page
Fig. 1.1	Polymerization behavior of silica in acidic and alkaline medium: a- acid catalyzed process with linear or randomly branched polymer; b- base catalyzed polymerization with highly branched cluster (Brinker and Scherer 1990)	8
Fig. 3.1	FT-IR spectra of RHA silica and metal modified silica catalysts: a- RHA-Al, b- RHA-In, c- RHA-Fe, d- RHA-SiO ₂ and e- RHA-Ga	41
Fig. 3.2	FT-IR spectra of gallium modified RHA with different loading of Ga ³⁺ : a- RHA 5%Ga, b- RHA-10%Ga and c- RHA-15%Ga	41
Fig. 3.3	²⁹ Si MAS NMR spectra of RHA silica samples synthesized by using NaOH of different concentrations: a- RHA-SiO ₂ (1M), b- RHA-SiO ₂ (2M), c- RHA-SiO ₂ (3M) and d- RHA-SiO ₂ (5M)	44
Fig. 3.4	²⁹ Si MAS NMR spectra of a- RHA-SiO ₂ , b- RHA-Al, c- RHA-Ga, d- RHA-In and e- RHA-Fe	45
Fig. 3.5	²⁷ Al MAS NMR spectra of RHA-Al: a- as synthesized and b- calcined	47
Fig. 3.6	⁷¹ Ga MAS NMR spectrum of RHA-Ga catalyst	48
Fig. 3.7	ESR spectrum (X-band) of RHA-Fe at room temperature	49
Figure 3.8	The N ₂ adsorption-desorption analysis data for various silica samples: a- N ₂ adsorption isotherms; b- The pore size distribution	51
Fig. 3.9	The N ₂ adsorption-desorption isotherms of RHA-Ga and RHA-Fe; Inset is the BJH pore size distribution of the respective catalyst	52
Fig. 3.10	The powder X-ray diffraction patterns of a- RHA-SiO ₂ , b- RHA-Al and c- RHA-Fe	57
Fig. 3.11	The powder X-ray diffraction patterns of a- RHA-5%Ga, b- RHA-10%Ga, and c- RHA-15%Ga	57
Fig. 3.12	The SEM Micrographs of a- RHA-SiO ₂ , b- RHA-Ga, d- RHA-10%Ga and e- RHA-15%Ga (Mag. 20k x)	59
Fig. 3.13	The TEM Micrographs of a- RHA-SiO ₂ and b- RHA-Fe	59

Fig. 4.1	The reaction profile of benzene and BC at 80 °C over RHA-Ga with different molar ratios of Bz/BC	75
Fig. 4.2	The reaction profile of benzene and BC over RHA-Ga at different temperatures using Bz/BC molar ratio of 15:1	77
Fig. 4.3	The reaction profile of Bz and BC at 80 °C over RHA catalysts with different loading of Ga ³⁺ ions using Bz/BC molar ratio of 15:1	79
Fig. 4.4	The reaction profile for the benzylation of Bz with BC at 80 °C over different catalysts using Bz/BC molar ratio of 15:1	81
Fig. 4.5	The reaction profile for the reaction between Bz and BC at 80 °C and Bz/BC molar ratio of 15:1 over the catalytic activity of RHA-Ga or gallium nitrate salt	84
Fig. 4.6	The pseudo-first order rate plot for benzene benzylation reaction (at 80 °C and Bz/BC molar ratio of 15:1) over RHA-In catalyst	87
Fig. 4.7	Arrhenius plots for the benzylation of benzene over different catalysts	87
Fig. 4.8	The effect of electron donating substituents for the benzylation of benzene over RHA-Ga for 90 min using molar ratio of 15:1	89
Fig. 4.9	The reaction profile for the benzylation of <i>p</i> -Xyl with BC at 80 °C over RHA-In using different molar ratios of <i>p</i> -Xyl/BC	99
Fig. 4.10	The reaction profile for the benzylation of <i>p</i> -Xyl with BC at different temperatures using <i>p</i> -Xyl/BC ratio of 15:1 and RHA-In catalyst	100
Fig. 4.11	The reaction profile for the benzylation of <i>p</i> -Xyl with BC at 80 °C using <i>p</i> -Xyl/BC molar ratio of 15:1 and RHA-In catalysts with different loading of indium ions	102
Fig. 4.12	The reaction profile for the benzylation of <i>p</i> -Xyl with BC at 80 °C and <i>p</i> -Xyl/BC molar ratio of 15:1 using RHA-In or Indium nitrate as a catalyst	104
Fig. 4.13	The reaction profile for the benzylation of <i>p</i> -Xyl with BC at 80 °C over different catalysts using <i>p</i> -Xyl/BC molar ratio of 15:1	106
Fig. 4.14	The reaction profile for the benzylation of <i>p</i> -Xyl and other aromatics (AR) at 80 °C with AR/BC molar ratio of 15:1 using RHA-Ga catalyst -Ga catalyst	108
Fig. 4.15	The reaction profile for the benzylation of different xylene isomers at 80 °C using Xyl/BC molar ratios of 15:1 and RHA-Fe catalyst	110

Fig. 4.16	The reaction profile for the benzylation of CB with BC at 90 °C over RHA-In catalyst using different molar ratios of CB/BC	118
Fig. 4.17	The reaction profile for the benzylation of CB with BC at different temp. using CB/BC molar ratio of 15:1 and RHA-In as a catalyst	120
Fig. 4.18	The catalytic profile of RHA catalysts of different loaded indium for the benzylation of CB with BC at 90 °C	123
Fig. 4.19	The reaction profile for the benzylation of CB at 90 °C over RHA-In or indium nitrate catalysts using CB/BC molar ratio of 15:1	125
Fig. 4.20	The reaction profile for the benzylation of CB with BC at 90 °C over different catalysts using CB/BC molar ratio of 15:1	127
Fig. 4.21	The pseudo-first order rate plot for chlorobenzene benzylation (at 90 °C and CB/BC molar ratio of 15:1) over RHA-Ga catalyst	129
Fig. 4.22	Arrhenius plots for the benzylation of chlorobenzene over RHA catalysts	130
Fig. 5.1	The reaction profile for the <i>tert</i> -butylation of Bz with TBC at 80 °C over RHA-In catalyst using different Bz/TBC molar ratios	142
Fig. 5.2	The reaction profile of RHA-In for the <i>tert</i> -butylation of Bz with TBC at different temperatures using Bz/TBC molar ratio of 15:1	145
Fig. 5.3	The reaction profile of different catalysts for the <i>tert</i> -butylation of benzene at 80 °C using Bz/TBC molar ratio of 15:1	147
Fig. 5.4	The reaction profile for the <i>tert</i> -butylation of Bz with TBC at 80 °C over RHA catalysts with different loading of indium ions using Bz/TBC molar ratio of 15:1	150
Fig. 5.5	The reaction profiles of iron nitrate and RHA-Fe catalysts for the <i>tert</i> - butylation of Bz with TBC at 80 °C using Bz/BC molar ratio of 15:1	152
Fig. 5.6	The first order rate plot for benzene <i>tert</i> -butylation reaction (at 80 °C and Bz/TBC molar ratio of 15:1) over RHA-Fe catalyst	154
Fig. 5.7	Arrhenius plots for the <i>tert</i> -butylation of benzene over different catalysts	155
Fig. 5.8	The reaction profiles for the <i>tert</i> -butylation of aromatics (AR) at 80 °C over RHA-Fe catalyst using AR/TBC molar ratio of 15:1	156
Fig. 5.9	The performance of RHA-Fe catalyst for the <i>tert</i> -butylation of different xylene isomers at 80 °C using Xyl/TBC molar ratio of 15:1	158

LIST OF SCHEMES

	Page
Scheme 1.1	14
Reaction scheme for the propylation of benzene with propylbromide, it shows the main product resulted from the rearrangement of the primary alkyl chain was the secondary alkylbenzene (Smith 2002)	
Scheme 3.1	43
The silica surface with silicon atoms of various bridging bonds	
Scheme 4.1	73
Reaction scheme for the benzylation of benzene with BC over RHA-Al, RHA-Ga, RHA-In and RHA-Fe	
Scheme 4.2	88
The trend of the catalyst reactivity for the benzylation of benzene and different substituted benzenes	
Scheme 4.3	91
The formation of the BC complex helped by dynamic adsorption on the RHA-M surface. The BC adsorbed complex will have a weaker C-Cl bond	
Scheme 4.4	92
The suggested mechanism by which the immobilized carbocation undergoes transformation when a substrate molecule comes close enough for the substitution reaction to take place. Once formed the primary products have restricted access to the catalyst surface limited by the size of the pores	
Scheme 4.5	97
Reaction scheme for the benzylation of xylenes with BC over RHA-Ga, RHA-In and RHA-Fe: a- <i>p</i> -Xyl, b- <i>o</i> -Xyl and c- <i>m</i> -Xyl	
Scheme 4.6	112
The expected positions for the electrophilic attack of benzyl carbocation at <i>o</i> -, <i>m</i> - and <i>p</i> -Xyl. Similar numbers on each molecule indicate for chemically equivalent carbon atoms	
Scheme 4.7	116
Reaction scheme for the benzylation of chlorobenzene with BC over the activity of RHA-Ga, RHA-In and RHA-Fe: a- Main reaction and b- Side reaction	
Scheme 5.1	141
Reaction scheme for the <i>tert</i> -butylation of aromatics with TBC over the activity of RHA-Al, RHA-Ga, RHA-In and RHA-Fe catalysts	

LIST OF SYMBOLS AND ABBREVIATIONS

A_m	-	Area occupied by the adsorbed molecule in the monolayer
An	-	Anisole
BC	-	Benzylchloride
BET	-	Brunauer, Emmett and Teller
BJH	-	Barret, Joyner and Halenda
Bz	-	Benzene
CB	-	Chlorobenzene
CMDPM	-	Chloromethyldiphenylmethane
CTBB	-	Chloro- <i>tert</i> -butylbenzene
DBB	-	Di-benzylbenzene
DBCB	-	Di-benzylchlorobenzene
CDPM	-	Chlorodiphenylmethane
DMDPM	-	Di-methyldiphenylmethane
DMTBB	-	Di-methyl- <i>tert</i> -butylbenzene
DPM	-	Di-phenylmethane
DTBB	-	Di- <i>tert</i> -butylbenzene
DTBT	-	Di- <i>tert</i> -butyltoluene
E_a	-	Energy of activation
EB	-	Ethylbenzene
EDX	-	Energy Dispersive X-ray spectroscopy
ESR	-	Electron Spin Resonance

FT-IR	-	Fourier Transform Infra-Red
HMS	-	Hexagonal Mesoporous Silica
ICP-MS	-	Inductively Coupled Plasma Mass Spectrometer
IUPAC	-	The International Union of Pure and Applied Chemistry
k	-	Reaction rate constant
K	-	Kelvin (absolute temperature unit)
MDPM	-	Methyldiphenylmethane
Mont.	-	Montmorillonite clay
MPA	-	Molybdenum Poly Acid
N	-	Avogadro's number.
P/P_0	-	Relative pressure
P_c	-	Critical pressure
P_0	-	Absolute pressure inside sample chamber (mm Hg)
RH	-	Rice husk
RHA	-	Rice husk ash
RHA-Al	-	Aluminum (5% loaded) supported on silica from RHA
RHA-Fe	-	Iron (5% loaded) supported on silica from RHA
RHA-Ga	-	Gallium (5% loaded) supported on silica from RHA
RHA-In	-	Indium (5% loaded) supported on silica from RHA
RHA-SiO ₂	-	Silica extracted from rice husk ash
S_{BET}	-	BET specific surface area (m ² g ⁻¹)
SEM	-	Scanning Electron Microscopy
²⁹ Si MAS NMR	-	²⁹ Si Magic Angle Spinning Nuclear Magnetic Resonance
SiO ₂	-	Silica
Si-OH	-	Silanol

Si–O–Si	-	Siloxane
TBB	-	<i>tert</i> -Butylbenzene
TBC	-	<i>tert</i> -Butylchloride
TBT	-	<i>tert</i> -butyltoluene
T _c	-	Critical temperature
TEM	-	Transmission Electron Microscopy
T _g	-	Glass transition temperature
TOF	-	Turn Over Frequency
Tol	-	Toluene
TPA	-	Tungstic Acid
TTBB	-	Tri- <i>tert</i> -butylbenzene
XRD	-	Powder X-ray Diffractometry
Xyl	-	Xylene
%	-	Percentage

LIST OF APPENDICES

	Page
Appendix A – FT-IR spectra	
A.1 FT-IR spectra of RHA silica samples prepared using NaOH solution of different concentrations: a- RHA-SiO ₂ (1M), b- RHA-SiO ₂ (2M), c- RHA-SiO ₂ (5M) and d- RHA-SiO ₂ (3M)	184
A.2 FT-IR spectra of indium modified RHA catalysts with different loading of: In ³⁺ : a- RHA-5%In, b- RHA-10%In and c- RHA-15%In	184
Appendix B – Nitrogen adsorption analysis	
B.1 The nitrogen adsorption isotherms of: a- RHA-Al and RHA-In, b- RHA-10%Ga and RHA-15%Ga, c- RHA-10%In and RHA-15%In; Insets are the pore size distribution of the respective samples	186
Appendix C – Powder XRD diffraction patterns	
C.1 The powder X-ray diffraction patterns of: a- RHA-5%In, b- RHA-10%In, and c- RHA-15%In	187
Appendix D – Electron microscopic analysis	
D.1 The SEM micrographs of: a- RHA-Al, b- RHA-In, c- RHA-Fe, d- RHA-10%In and e- RHA-15%In	188
D.2 The TEM micrographs of: a- RHA-Al, b- RHA-Ga and c- RHA-In	189
D.3 The EDX spectra of: a- RHA-SiO ₂ , b- RHA-Al, c- RHA-Ga, d- RHA-In, and e- RHA-Fe	190
Appendix E – First order rate plots	
E.1 The pseudo first order rate plots for benzene benzylation (at 80 °C and Bz/BC molar ratio of 15:1) over: a- RHA-Ga and b- RHA-Fe	191
E.2 The pseudo first order rate plots for the benzylation of: a- toluene and b- p-xylene at 80°C over RHA-Ga using aromatic/BC molar ratio of 15:1	192
E.3 The pseudo first order rate plots for chlorobenzene benzylation (at 90 °C and CB/BC molar ratio of 15:1) over: a- RHA-In and b-	193

RHA-Fe

E.4	The first order rate plots for benzene <i>tert</i> -butylation (at 80 °C and Bz/TBC molar ratio of 15:1) over: a- RHA-Ga and b-RHA-In	194
E.5	The first order rate plots for <i>tert</i> -butylation of aromatics (at 80 °C and aromatic/TBC molar ratio of 15:1) over RHA-Fe: a- toluene, b- chlorobenzene and c- <i>o</i> -xylene	195

Appendix F – GC analysis data

F.1	GC chromatogram for the mixture of benzene benzylation reaction: a- before reaction and b- after reaction	196
F.2	GC chromatogram for the mixture of <i>m</i> -xylene benzylation reaction: a- before reaction and b- after reaction	196
F.3	GC chromatogram for the mixture of chlorobenzene benzylation at the earlier stages of the reaction process (obtained by GC-MS)	197
F.4	GC chromatogram for the mixture of benzene <i>tert</i> -butylation reaction: a- before reaction and b- after reaction	197
F.5	GC chromatograms for the mixtures of <i>tert</i> -butylation reaction of aromatics (after reaction): a- toluene, b- <i>o</i> -xylene, c- <i>m</i> -xylene, d- <i>p</i> -xylene and e- chlorobenzene	198

Appendix G – GC-MS analysis data

G.1	GC-MS data for the products of benzene benzylation reaction	199
G.2	GC-MS data for the products of toluene benzylation reaction	201
G.3	GC-MS data for the products of <i>o</i> -xylene benzylation reaction	202
G.4	GC-MS data for the products of <i>m</i> -xylene benzylation reaction	204
G.5	GC-MS data for the products of <i>p</i> -xylene benzylation reaction	206
G.6	GC-MS data for the products of chlorobenzene benzylation reaction	209
G.7	GC-MS data for the products of benzene <i>tert</i> -butylation reaction	211
G.8	GC-MS data for the products of toluene <i>tert</i> -butylation reaction	212
G.9	GC-MS data for the products of <i>o</i> -xylene <i>tert</i> -butylation reaction	213
G.10	GC-MS data for the products of <i>p</i> -xylene <i>tert</i> -butylation reaction	214
G.11	GC-MS data for the products of <i>m</i> -xylene <i>tert</i> -butylation reaction	215

**ALUMINUM, GALIUM, INDIUM DAN FERUM YANG DISOKONG DI
ATAS SILICA ABU SEKAM PADI SEBAGAI MANGKIN BAGI TINDAK
BALAS PENGALKILAN FRIEDEL-CRAFTS SEBATIAN AROMATIK**

ABSTRAK

Mangkin RHA-Al, RHA-Ga, RHA-In dan RHA-Fe telah disediakan dengan mengubahsuai permukaan silika abu sekam padi (RHA) dengan menggunakan ion Al^{3+} , Ga^{3+} , In^{3+} dan Fe^{3+} . Mangkin pepejal yang telah disintesis menunjukkan tekstur dan struktur yang baik seperti yang disahkan oleh teknik-teknik fiziko-kimia seperti FTIR, ^{29}Si NMR, NMR fasa pepejal dan ESR untuk nukleus logam, XRD, penjerapan N_2 , SEM-EDX, TEM dan analisis ICP-MS. Aktiviti mangkin tersebut terhadap pembenzilan benzena dan beberapa benzena tertukar ganti dengan benzilklorida (BC) dipengaruhi secara positif oleh peningkatan suhu tindak balas, jisim mangkin dan peratus muatan spesis aktif. Walau bagaimanapun, peningkatan nisbah molar aromatik terhadap BC menunjukkan kesan negatif terhadap aktiviti mangkin tersebut. Mangkin RHA-Fe menunjukkan aktiviti pemangkinan yang paling tinggi manakala mangkin RHA-Ga dan RHA-In menunjukkan darjah pemilihan yang paling tinggi terhadap difenilmetana (DPM) dan terbitannya (contoh: produk mono benzil). RHA-Al didapati tidak menunjukkan sebarang aktiviti dalam tindak balas tersebut. Tindak balas benzena mono tertukar ganti dengan agen pelepas elektron didapati bertentangan dengan ciri-ciri klasik tindak balas pembenzilan Friedel-Craft menggunakan mangkin asid. Kereaktifan terhadap benzena tertukar ganti seperti *p*-xilena didapati berpadanan dengan benzena. Kereaktifan isomer-isomer xilena adalah seperti turutan berikut: *o*-xilena > *m*-xilena > *p*-xilena. Pemilihan terhadap hasil dimetildifenilmetana (DMDPM) berkurang

mengikut turutan berikut: *m*-xilena > *p*-xilena > *o*-xilena. Logam garam nitrat yang tidak disokong (kecuali aluminium nitrat) menunjukkan aktiviti sangat baik berbanding mangkin logam yang disokong tetapi menghasilkan banyak produk sampingan dibenzil. Tindak balas pembutilan-*tert* (menggunakan *tert*-butil klorida) benzena dan benzena tertukar ganti diuji dengan menggunakan mangkin RHA. Mangkin RHA-Fe menunjukkan aktiviti pemangkinan yang paling tinggi manakala RHA-Ga menunjukkan darjah kereaktifan dan pemilihan yang paling rendah. RHA-In menunjukkan darjah pemilihan yang tertinggi terhadap *tert*-butilbenzena (TBB) dan terbitannya. Sebaliknya, RHA-Al adalah hampir tidak aktif. Aktiviti pemangkinan bagi semua mangkin tersebut dilihat menunjukkan kesan positif terhadap peningkatan muatan ion logam, nisbah molar Bz/TBC dan suhu tindak balas. Logam garam nitrat yang tidak disokong didapati kurang efektif dan kepilihan berbanding dengan logam yang disokong. Keaktifan mangkin dalam tindak balas pembutilan-*tert* aromatik adalah seperti turutan berikut: : *o*-xilena > benzena > toluena > klorobenzena. Bagi isomer xilena yang berlainan, kereaktifan dan pemilihannya berkurang mengikut turutan berikut: *o*-xilena > *m*-xilena > *p*-xilena. Kesemua mangkin RHA adalah stabil terhadap larut lesap dan boleh digunakan berulang kali tanpa sebarang perubahan yang signifikan dalam proses pembenzilan tetapi mengalami penurunan yang ketara selepas digunakan sebanyak dua pusingan dalam tindak balas pembutilan-*tert*.

ALUMINUM, GALLIUM, INDIUM AND IRON SUPPORTED ONTO RICE HUSK ASH SILICA AS CATALYSTS FOR THE FRIEDEL-CRAFTS ALKYLATION REACTIONS OF AROMATIC COMPOUNDS

ABSTRACT

The heterogeneous catalysts derived from rice husk ash (RHA) silica were prepared by modifying the surface of silica extracted from RHA with Al^{3+} , Ga^{3+} , In^{3+} and Fe^{3+} ions. The catalysts were labeled as RHA-Al, RHA-Ga, RHA-In and RHA-Fe, respectively. The as-synthesized solid catalysts showed good textural and structural properties as it was confirmed by the physico-chemical techniques such as FT-IR, ^{29}Si MAS NMR, solid-state NMR and ESR for metal nuclei, powder XRD, N_2 -adsorption, SEM-EDX, TEM and ICP-MS elemental analysis. The activity of the catalysts for the benzylation of benzene and some substituted benzenes with benzylchloride (BC) was observed to be positively influenced with increasing reaction temperature, catalyst weight and percentage loading of active species. However, it was negatively affected with increasing aromatic to BC molar ratio. The highest catalytic activity was registered over RHA-Fe whereas the highest selectivity for the diphenylmethane (DPM) and its derivatives (i.e. mono benzylated products) was obtained from RHA-In. However, RHA-Al was found completely inactive. The activity for benzylation of mono-substituted benzenes with an electron releasing substituents was found to oppose the classical acid catalyzed Friedel-Crafts type benzylation reactions. The reactivity towards disubstituted benzenes such as *p*-xylene was found to be comparable to that of benzene. Whereas, that among different xylene isomers followed the order: *o*-xylene > *m*-xylene > *p*-xylene. However, the selectivity for dimethyldiphenylmethane (DMDPM) products decreased as follows: *m*-xylene > *p*-xylene > *o*-xylene. The un-supported metal

nitrates (except aluminum nitrate) showed superior activity over the supported metal catalysts but larger amounts of dibenzylated side products were formed. The *tert*-Butylation reactions (using *tert*-butylchloride) of benzene and some substituted benzenes were tested over RHA catalysts. The RHA-Fe catalyst showed the highest activity whereas RHA-Ga exhibited the lowest reactivity and selectivity. RHA-In gave the highest selectivity to *tert*-butylbenzene (TBB) and TBB derivatives. In contrast, RHA-Al was almost inactive. The catalytic performance of the catalysts was observed to be positively affected by increased loading of metal ions, Bz/TBC molar ratio and temperature. Un-supported metal nitrates were found less effective and selective than the respective supported ones. For the *tert*-butylation of other aromatics, the activity of the catalysts decreased in the order: *o*-xylene > benzene > toluene > chlorobenzene. However, for different xylene isomers, both activity and selectivity decreased in the order *o*-xylene > *m*-xylene > *p*-xylene. All RHA catalysts were stable against leaching and were reused for the alkylation reactions several times without any significant change in their performance for the benzylation, but with an obvious decrease for *tert*-butylation after more than two cycles.

Chapter 1

Introduction

In recent years, environmental and economic considerations have raised strong interest to redesign commercially important processes so that the use of harmful substances and the generation of toxic waste could be avoided or minimized. In this respect, there is no doubt that heterogeneous catalysis can play a key role in the development of environmentally benign processes in petroleum chemistry and in the production of fine chemicals particularly through the alkylation reaction by replacing the most hazardous conventional Brønsted and Lewis acids.

Many porous materials have been intensively studied (and are discussed in chapter 4 and 5) for this purpose as solid acid catalyst i.e. zeolites, clays, super solid acids etc., or as a support for Lewis and/or Brønsted acids such as silica, alumina, zeolites, mesoporous materials, clays, synthetic polymers, resins etc. The reactivity of heterogeneous catalysts was found different and depends on many factors. However, the most important factors include: the nature of support and its textural properties, the type of acid introduced, the mode of synthesis. It is also important to highlight that as long as the heterogeneous catalyst is used for the alkylation reaction involves alkyl halide as alkylating agent; the acidity of the catalyst was found not to be the keyword of the activity as usually observe for the conventional Frieda-Crafts reactions. Rather, the reactivity may depend on the reduction potential of the bonded metallic species. However, for many alkylation reactions, the combination of both gives extra advantageous.

It is well known that mesoporous silica based catalysts though suffer from the lack of acidity, but the larger pore diameters (Corma 1997) of these catalysts makes them highly active in the alkylation reactions when compare to strong solid acid catalysts such as zeolite based catalysts. Nevertheless, conventional amorphous silica based catalysts are characterized with rather large average pore diameters; they were far behind in this rivalry and in many cases they were almost inactive. The lack of activity is attributed to the relatively lower surface area and the deficiency and/ or instability of supported active species as well as the undefined pore systems of these materials. Nowadays, development of catalysts based on amorphous silica with good textural properties and excellent catalytic performances is become a challenging goal. Considering the fact that amorphous silica can be synthesized easily at ordinary conditions via the sol-gel process. In addition the mild acidity of amorphous silica is expected to resist the deactivation that is usually accompanied the use of strong solid acid catalysts such as zeolites. Since over the surface of these weak acidic catalysts frail adsorption of products is expected and hence faster diffusion of the bulky products formed.

The major precursors used for the production of amorphous silica are alkoxysilane compounds such as tetra ethyl orthosilicate (TEOS) and tetra methyl ortho silicate (TMOS). However, the use of these organosilicon chemicals is accompanied by many hazardous effects to human health (Nakashima et al. 1998). Based on this, searching for a cheaper source with less risk effect is even become more demandable. RHA is considered one of these sources. The processes of fabricating catalysts from RHA can be followed easily using simple and less hazardous inorganic chemicals at ordinary conditions. The catalysts which were

synthesized from RHA silica via the sol-gel technique exhibited textural properties comparable to many conventional synthetic porous materials. Moreover, the supported metals in these catalysts are very stable and impart an excellent catalytic activity to RHA silica material.

Noteworthy, an important line of research has focused on the enlargement of the pore sizes into larger diameters, allowing larger molecules to enter the pore system, to be processed there and to leave the pore system again. Therefore, heterogeneous catalysts based on RHA silica are considered promising in different industrial applications because they can offer this requirement. Indeed, in contrast to zeolites and ordered mesoporous silica, RHA-SiO₂ or metal modified silica do not have that short-range of pore ordering of the former materials. They are rather; present a long-range order, similarly to silica-alumina. However, their acidity is weaker than that of silica-alumina. Actually, similar to ordered mesoporous silica, they are almost not acidic. Interestingly, their large pores allow them to process more feeds and to accommodate larger molecules as *tert*-butylated aromatic compounds as we will discuss this latter.

1.1 Silica

1.1.1 The occurrence of silica

The name silica comprises a large class of products with the general formula SiO₂ (anhydrous silica) or SiO₂.xH₂O (hydrated silica). Silica is a naturally occurring substance and it is considered the most abundant material on earth since 55 % w/w of the earth's surface consists of either silica or silicates (Scott 1993). Naturally, silica occurs in minerals, such as quartz and flint and in plants such as

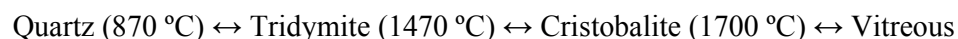
bamboo, rice and barley (Vasant *et al.* 1995). However, most of the silica used in chemical applications has a synthetic origin.

1.1.2 Surface species of silica

The ultimate particles, which make up the silica, can be regarded as polymers of silicic acid, consisting of interlinked SiO_4 tetrahedra. At the surface, the structure terminates in either Si-O-Si with oxygen on the surface, or one of the several forms of silanol groups (Si-OH). The silanols can be divided into isolated (free silanols), vicinal (bridged silanols) and geminal silanols (two hydroxyl groups attached to one Si atom). In almost all amorphous silica, there are internal silanol groups throughout the particle structure (intraglobular) in addition to the surface silanols. Such intraglobular silanols are inaccessible to water. Davydov *et al.* (1964) estimated the concentration of intraglobular silanol for a silica gel to be 0.5 mmol g^{-1} , after the silica sample had been treated at 200°C . A temperature higher than 600°C was required to remove all these silanol species.

1.1.3 Types and phases of silica

Silica exists naturally in both crystalline and amorphous forms, but the majority is crystalline (Iler 1979). Crystalline silica occurs in various structures, but the most common forms are quartz, cristobalite and tridymite. According to Vasant *et al.* (1995) and Scott (1993), the transformations between the three common crystalline forms and amorphous vitreous silica glass can be illustrated as follows:



Amorphous silica, found as opal and infusible earth in nature. It has no regular structure and exhibits a higher degree of hydration than crystalline forms (Gregg and Sing 1982). Amorphous silica is abundant in various forms include fibers, sheets, sols, gels and powders. According to Iler (1979) amorphous silica is considered to contain three main types' i.e. vitreous silica (made by fusing quartz), silica M (formed by irradiating with high speed neutrons) and micro-amorphous silica (includes sols, gels, powders, and porous glasses). With respect to their dispersity however, amorphous silica is available in various forms i.e. soluble silica, silica sols, hydrogels, xerogels, aerogels, and precipitated silica (Vasant *et al.* 1995). Because the porosity of amorphous silica introduces a large surface area inside the silica particles and because all adsorption and catalysis processes require a large surface area, amorphous silica is far more interesting for these applications than its counterpart, i.e. the crystalline silica. However, different surface properties can be achieved by changing the method of preparation as well as some specific parameters during the synthesis of amorphous silica.

Colloidal silica is an important type of amorphous silica and is known as silica sol. Silica sols are synthesized by mixing silicate salts with an acid. The most documented method for preparing silica sols is the sol-gel route (Brinker and Scherer 1990). In this process as we'll see latter, mono silicic acid molecules " Si(OH)_4 " condense to form a siloxane network. However, the sols are produced by the formation of stable particles of colloidal size as a result of the condensation process. Soluble silicate (mainly sodium salt) has commonly been used as the starting compound (Vasant *et al.* 1995, Unger 1979 and Barby 1976). But over the last decades the use of alkoxysilanes Si(OR)_4 , ($\text{R} = \text{CH}_3, \text{C}_2\text{H}_5 \text{ or } \text{C}_3\text{H}_7$) has rapidly

gained importance (Stöber *et al.* 1968). The rate of the condensation process can be controlled by changing the pH and addition of electrolytes to favor either the growing of particles or linkage of the particles to form chains. The condensation proceeds until the elastic stress point is reached (gelation point), when the sol has condensed to a gel.

Silica gels are coherent, rigid and comprised of three dimensional networks of contiguous particles of colloidal silica. The as-formed gel is termed a hydrogel and its structure is controlled by many parameters i.e. the temperature, pH, the nature of the solvent, the nature of added electrolyte and the type of starting silicate.

Silica xerogel is formed when the hydrogel losses its pore filling liquid (mainly water) by capillary force during the drying process. It is formed with porosity and surface area depending on the conditions of this process. However, aerogel is formed when the water in the pores of the hydrogel is replaced with a suitable solvent and then this solvent is removed from the pores during the drying process by heating above the solvent critical temperature (T_c) and pressure (P_c). By this process, the problems associated with cracking and shrinking of xerogel are avoided or reduced because there is no liquid-vapor interface and no capillary pressure. Aerogels have pore volume higher than the corresponding xerogel and similar to that of the original sol.

Precipitated silica includes a wide range of silica with a variety of structural characteristics. It was defined by Barby (1976) as dry silica with no long or short distance characteristic structure. The formation of this type occurs when the ultimate

silica particles are coagulated as loose aggregates in the aqueous medium. The coagulation however, may be affected by high salt concentration or other coagulants. The properties of precipitated silica may therefore be supposed to be similar to those of the gel.

Pyrogenic silica (anhydrous silica) is synthesized by heating the silica at elevated temperature using different processes. According to the method of preparation, various types of pyrogenic silica can be obtained which include fumed silica, arc silica and plasma silica. Fumed silica (aerosol) is most widely used as a source of pure silica. It is produced by burning SiCl_4 with hydrogen and oxygen as illustrated in equation 1.1. The preparation process of fumed silica involves linking of the primary particles into a linear chain to form a nonporous structure.



Arc silica is formed by reduction of highly-pure sand at high temperature. It consists of particles with various sizes. Primary particles in this case agglomerate in spheres and do not form chains. Because of the dense packing of the particles, these spheres do not show any porosity. The specific surface is the external surface of the spheres. Plasma silica is produced by volatilization of purified sand in a plasma jet. The product is ultra fine silica powder.

1.1.4 The sol-gel process

Sol-gel process is a wet chemical method. It involves the transition of a system from a liquid “sol” (mostly colloidal suspension) into a solid “gel” phase.

The sol-gel technique is an appropriate method to produce pure and homogeneous product at a very low temperature; therefore it is useful for the preparation of most of the ceramic and glass materials. This technique has been widely used to synthesize silica xerogels (Brinker and Scherer 1990 and Brinker 1990) and aerogels (Fricke and Emmerling 1998) from appropriate precursors (silicate salts or alkoxysilanes). In a typical sol-gel process, the precursor is subjected to a series of processes including hydrolysis, condensation, gelation, aging and drying.

Hydrolysis and condensation usually occur simultaneously. It was reported by Ying *et al.* (1973) and Ro and Chung (1991) that the relative rate of these processes as well as the structure of the gel produced are significantly influenced by the pH of the reaction. In acidic medium weakly branched polymeric networks are formed and the gels show slit-shaped micropores and have a fibrous or plate-like structure (Vasant *et al.* 1995 and Iler 1979). In basic medium on the contrary, highly branched networks with ring structure are formed and the gel is characterized by cylindrical pores and spherical particles (Vasant *et al.* 1995 and Iler 1979). The structures are illustrated in Fig. 1.1.

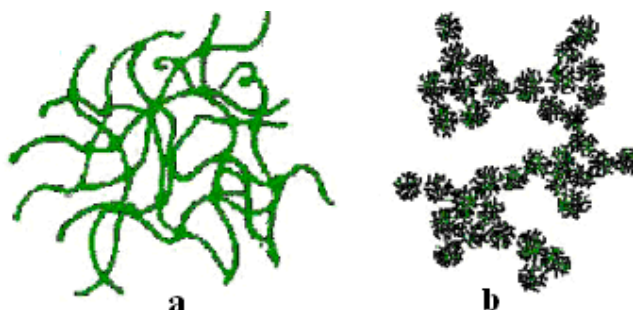
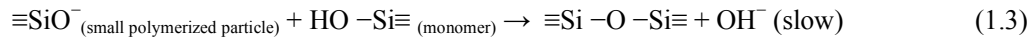


Fig. 1.1: Polymerization behavior of silica in acidic and alkaline medium: a- acid catalyzed process with linear or randomly branched polymer; b-base catalyzed polymerization with highly branched cluster (Brinker and Scherer 1990)

The condensation and polymerization of Si(OH)_4 species is not analogous to the linear branching and cross-linking in organic polymers. Iler (1979) differentiated three pH domains in the polymerization process. At $\text{pH} < 2$ the formation and aggregation of primary particles occur together. However, in this region Ostwald ripening contributes little to growth after particles exceed 2 nm in diameter, thus developing gel networks are composed of exceedingly small primary particles (Brinker and Scherer 1990). At pH 2 the isoelectric point is reached and above this point the condensation preferentially occurs between more highly condensed species and those less highly condensed and somewhat neutral species. Cyclization occurs and particle growth stops when the particles reach 2-4 nm in diameter (Keefer 1990). The reaction is proposed to proceed as follows:



At pH above pH 7, particles are charged by ionization. Accordingly aggregation is reduced. Growth of particle in this region occurs by monomer deposition and Ostwald ripening (Brinker and Scherer 1990). At this pH range, condensed species are ionized and therefore, mutually repulsive. Growth occurs primarily through the addition of monomers to the more highly condensed particles rather than by particle aggregation. Accordingly, particles grow in size and decrease in number. Following the arrangement of Murakata *et al.* (1992), the pore size distribution at this region is controlled by the addition of several kinds of inorganic salts and surfactants in the sol-gel reaction mixture. Aggregation can only take place by the addition of salt because it reduces the double layer thickness. The addition of inorganic salt depresses the formation of mesopores.

The gel is formed when the polymeric network extends throughout the total volume. The point at which a sol thickens to a gel is known as the gelation point t_{gel} . The gelation point is influenced by so many factors i.e. size of the container, solution pH, salt concentration, type of anion and solvent used. Controlling of the gelation rate however, is very important because it influences the pore structure. Fast gelation gives an open structure, because the particles are quickly connected and do not undergo further rearrangements.

Aging process is followed by keeping the gel in contact with the pre-filling liquid. In this stage, structure and properties of the gel keep changing as a function of time. During the aging, certain processes take place and cause significant changes in the pore structure and the surface area of the gel. The mechanisms by which these changes take place include poly-condensation, syneresis, coarsening and phase transformation (Brinker *et al.* 1982 and Matijević 1986). Interestingly, aging before drying was found to strengthen the network and thereby reduce the risk of fracture (Zarzycki *et al.* 1982).

The drying process is to convert the hydrogel into a xerogel. The conversion happens through three main stages: constant rate period, critical point and falling rate period. In the constant rate period, the greatest changes in volume, weight and density of the gel as well as shrinkage take place. Whereas at the critical point period, no further compression of network takes place but cracking is most likely occurred. However, the structure of the xerogel does not change in the falling rate period.

The structural changes that occurred during aging have an important effect on the drying process. It was found that aged gels were shrunk and crack less, because the high stiffness and strength of their networks provide higher ability to withstand the capillary pressure. The super critical drying is followed by removing the pore liquid above its critical point to avoid or to reduce the problems resulting from the capillary pressure, i.e. shrinking and cracking. Kistler (1932) reasoned that the problems of cracking and shrinking could be avoided by removing the liquid from the pores above the critical temperature (T_c) and critical pressure (P_c) of the liquid. In this process a sol or wet gel is placed into an autoclave and heated, once the critical point is passed, the solvent is vented at a constant temperature ($> T_c$). The resulting gel, called an aerogel has a volume similar to that of the original sol. However, the density of silica aerogel is similar to that of xerogel, i.e. $\sim 2 \text{ g cm}^{-3}$. Carbon dioxide (CO_2) which is characterized by lower critical point [$T_c = 31 \text{ }^\circ\text{C}$, $P_c = 7.0 \text{ MPa}$] is frequently used to exchange the pore liquid. Although the supercritical drying eliminates the capillary pressure, it does not completely eliminate shrinkage, because solid-vapor interfaces created at the final stage of this process can cause weakly condensed gels to shrink up to 50 % (Eyraud *et al.* 1988). The large scale structure of aerogel was found weak and easily collapsed by capillary pressure. Kistler (1932) reported that when an aerogel is immersed in a liquid, its structure collapses immediately after it has been subsequently dried.

1.1.5 Activation and de-activation of silica surface

The activation of silica surface can be achieved by dehydration of physisorbed water as well as by rehydroxylation which is the recovery of surface silanol (Si-OH). The deactivation process is carried out by the dehydroxylation of

surface silanol to form siloxane bonds (Si-O-Si). It is generally agreed that heating at 100 °C for a prolonged period, removes all physisorbed water on non-porous silica. Whereas, heating up to 200 °C is not necessarily adequate to remove all physisorbed water from the micropores of the porous silica (Unger 1979). It was also found that in the temperature range 200 – 400 °C, mainly vicinal OH condense, whereas in the region above 400 °C mainly isolated OH are expected to condense with increasing difficulty. However, temperatures > 1200 °C are required to remove all silanols (Agzamkhodzhaev *et al.* 1969).

Rehydroxylation is more difficult than the reverse process and requires a long time to be completely achieved. However, the rate and possibility of recovering depends on the temperature and time of dehydroxylation process. It was observed that complete rehydroxylation of the surface can only be achieved for SiO₂ which were heated to below 400 °C, but if it was calcined at higher temperature, only partial recovery of OH is achieved (Peri and Hensley 1968).

1.1.6 Structures of porous xerogels and aerogels

Porosity develops due to additional cross-linking or neck formation, the gel network becomes sufficiently strengthened to resist the compressive forces of surface tension. Thus the structure of the dried xerogel will be contracted and becomes a distorted version of the structure originally formed in solution. Porosity often exists on two length scales, i.e. within clusters “microporosity” and between clusters “mesoporosity”. For non aggregated mono dispersed system, the pore volume of the xerogels depends only on the particle-packing geometry and the pore size increases with the particle size. However, for aggregated systems, both the pore

volume and pore size depend on the aggregate structure. Compared to xerogels, aerogels have expanded structures that are often more closely related to the structure of the gel that existed at the gel point. However, for all categories of gels, aging prior to solvent extraction can alter the porosity of the dried product (Vasant *et al.* 1995). For instance the process of Ostwald ripening has the effect of strengthening the gel so that it stops shrinking earlier in the drying process. Conversion of xerogel to dense stable, solid materials by further thermal treatment lead to structural evolution as a consequence of dehydration, de-hydroxylation and sintering. The skeletal phase of the gel was observed to be evolved through continued condensation reactions when heated to temperature far below its melting point. The gel produced is found to be highly condensed, more or less homogeneous and often contains excess free volume. As the gel is heated to a near glass transition temperature, T_g , its skeletal structure approaches that of conventional glass made by melting.

1.2 Friedel –Crafts reaction

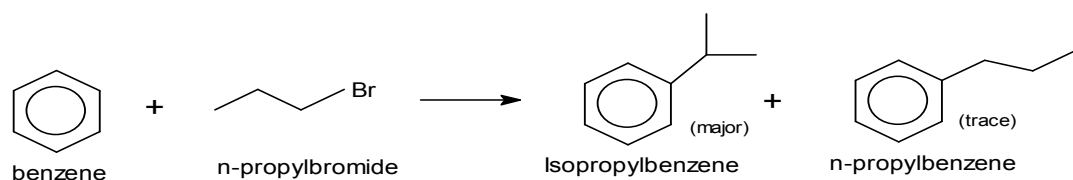
1.2.1 Back ground

Friedel–Crafts alkylation reaction is a typical electrophilic aromatic substitution and involves initially the formation of complex intermediates, i.e. “ σ - or π - complexes” between the alkyl halide and the metal halide catalyst (Bansal 1978). This reaction is also considered to be a nucleophilic substitution reaction, because it involves a nucleophilic attack by aromatic ring on the alkyl group (Morrison and Boyd 1973). The first typical Friedel-Crafts alkylation reaction was the reaction of benzene (aromatic) with amyl chloride (alkylating agent) in the presence of $AlCl_3$ to produce amylbenzene. This reaction was exclusively carried out by Charles Friedel

and his American collaborator James Mason Crafts in Paris in 1877 (Roberts and Khalaf 1984).

The most important alkylating agents are alkyl halides, alkenes and alcohols; but many other types of reagents have also been employed (Olah and Molnár 2003). The reactivity of Friedel - Crafts alkylation is based on these alkylating agents. For alkyl halides, the reactivity was found to decrease in the order Allylic ~ benzylic > tertiary > secondary > primary (Smith and March 2001).

One of the synthetic limitations of Friedel-Crafts alkylation reaction is the rearrangement of the alkylating reagent before it attacks the aromatic ring. Smith (2002) illustrated that, this rearrangement occurs by migration of H^- and R^+ . It is mainly observed for the primary alkyls (scheme 1.1) and usually it takes place in the order $1^\circ \rightarrow 2^\circ \rightarrow 3^\circ$.



Scheme 1.1: Reaction scheme for the propylation of benzene with propylbromide, it shows the main product resulted from the rearrangement of the primary alkyl chain was the secondary alkylbenzene (Smith 2002)

Gilman and Meals (1943) concluded that the isomerization of alkyl groups depends on the alkyl halide used and according to them the alkylation of benzene with primary alkyl halides gives primary and secondary alkylbenzenes as products. However, the amount of the latter increases at higher reaction temperatures. The secondary alkyl halides and tertiary alkyl halides however, yield secondary and tertiary alkyl benzenes respectively. The same phenomenon was also observed by

Schmerling and West (1954). They reported that primary alkyl chlorides produce primary and secondary alkyl benzenes and also tertiary alkyl benzenes if a tertiary hydrogen atom is available on the chain. They also found that the nature of the catalyst is decisive in the formation of secondary or tertiary alkylbenzenes.

Another synthetic limitation of Friedel-Crafts alkylation is the degradation and polymerization of the electrophile before attacking the aromatic substrate. Campbell Jr. and Spaeth (1959) and Shen *et al.* (1990) reported that the alkylating agent is degraded and polymerized before it can attack the deactivated aromatic substrate. This problem makes the alkylation of aromatics which contain meta-directing substituent extremely difficult or even not possible.

Many aromatics beside benzene and substituted benzenes can be alkylated by Friedel-Crafts reaction. These include fused ring compounds like naphthalene. Smith (2002) stated that some aromatics containing OH, OR, NH₂ substituents (except phenols) were found not to facilitate this reaction. This unusual behavior was assigned to the capability of the Lewis acid sites on the catalyst to coordinate with these aromatics, thereby making the catalyst ineffective.

1.2.2 Orientation and reactivity

Friedel-Crafts reaction proceeds when the electrophilic carbonium ion attacks the aromatic ring nucleophile since the ring has a high electron density. However, the departing group (H⁺) leaves without its electron pair (Bansal 1978). Morrison and Boyd (1973) reported that the reactivity for this reaction is generally dependent on the stability of the carbonium ion formed. Accordingly, the order of

reactivity of alkyl halides was found to follow the order of stability of carbonium ions. However, the order of reactivity of alkyl halide was found to decrease as follows, RX in allyl, Benzyl $> 3^\circ > 2^\circ > 1^\circ > CH_3X$. In benzene, the 6 hydrogen atoms are chemically equivalent and the electrophilic attack would give rise to a single product only. But if a substituent group is already occupying a position in the ring (e.g. toluene, xylenes, ethyl benzene, anisole, chlorobenzene etc.), the hydrogen atoms become non equivalent. Therefore the incoming electrophile may be directed primarily to *o*-, *m*- or *p*- positions depending on the substituent group. The substitution rate may be slower or faster than that of benzene. The group already on the ring determines the position and the rate of reaction and hence the products are often kinetically and not thermodynamically controlled (Bansal 1978). Two types of substituting groups are considered, activating (electron releasing) and de-activating (electron withdrawing) groups (Morrison and Boyd 1973).

Electron releasing group increases the substitution rate by activating all the positions in the benzene ring, but extra activation is given to *ortho* and *para* positions. Two types of activating group are categorized, the first type constitutes those containing an unshared pair of electrons on the atom connected to the ring e.g. O^- , NR_2 , NHR , NH_2 , OH , OR , $NHCOR$, $OCOR$, SR and halogens. The other type comprises substituents that lack an unshared pair of electrons on the atom connected to the ring e.g. Ar , R and COO^- . The substituting groups in the first type and due to the combination of resonance and (+*I*) field effects are expected to activate *ortho* and *para* much more than *meta* position. Halogens in contrast, possess (-*I*) field effect and hence they are considered deactivating substituents. However, the predominating resonance effect on halo benzenes favor the orientation towards *ortho*

and *para* rather than *meta* positions, though the registered substitution rates were less than in the case of benzene. The activating behavior of aryl group in the second category is explained by the fact that the lone pair of electrons from the aromatic sextet is playing the part played by the unshared pair (Smith and March 2001). While in case of alkyl group it is attributed to the hyper-conjugation observed in some canonical forms (Morrison and Boyd 1973). In case of COO^- substituent, its activating manner is assigned to its ability to donate through the (+I) field effect (Smith and March 2001).

Electron withdrawing group decreases the substitution rate by de-activating all the positions in the ring, but extra deactivation is given to *ortho* and *para* positions. This category contains the following substituents NR_3^+ , NO_2 , CF_3 , CN , SO_3H , CHO , COR , COOR , CONH_2 and any group which has positive charge. These substituents lack an unshared pair of electrons on the atom connected to the ring and hence have (-I) field effect. Furthermore, except NR_3^+ , which favors *para* orientation, all these substituents are primarily *meta* directors.

The proportion of *ortho* and *para* products in a reaction involving substituted benzenes differ widely but the factors that affect the reactivity at these positions are not well understood. Many factors are expected to have a significant influence on the product ratio; these include: steric, solvent and polar effects. Steric effect originates from both the group already present on the aromatic ring as well as the attacking reagent. As the size of the electrophile increases, the yield of the *ortho* isomer decreases e.g. $\text{CH}_3 > \text{C}_2\text{H}_5 > \text{CH}(\text{CH}_3)_2 > \text{C}(\text{CH}_3)_3$. The presence of various types of solvents (polar and non-polar) was also found to affect the reactivity of

electrophilic substitution reactions significantly. The effect of the electronic nature of the substituents (polar effect) is very significant, but this effect is more obvious in the case of electron-withdrawing groups because the *ortho* position has been deactivated.

1.2.3 Catalysts

Catalysts are substances or mixtures of substances that are effective to modify the rate of reactions carried out in vitro or in vivo (Prettre 1963). Depending on whether the catalyst and all the reactants belong to a single phase or not, it can be divided into two categories, i.e. *homogeneous* and *heterogeneous* catalyst. For Friedel-Crafts alkylation reactions and regardless of the type of alkylating reagent used, a catalyst is nearly always required. However, a few exceptional cases in which alkylation of aromatics were achieved without a catalyst have been reported (Olah and Nishimura 1974; Stang and Anderson 1978).

1.2.3.1 Homogeneous catalysts

Homogeneous catalysts such as anhydrous aluminum and ferric chlorides are the most frequently used for the conventional Friedel-Crafts reactions. Some other Lewis acid catalysts are also involved in this reaction i.e. AlBr_3 , BF_3 , GaBr_3 , etc. (Olah 1964 and Sharman 1962). The acidic strength of the most common Lewis acids decreases in following order $\text{BX}_3 > \text{AlX}_3 > \text{FeX}_3 > \text{GaX}_3 > \text{SbX}_5 > \text{InX}_3 > \text{SnX}_4 > \text{AsX}_5 > \text{SbX}_3 > \text{ZrX}_4$ (Smith 2002). However, among alkyl halides the reactivity decreases in the order $\text{F} > \text{Cl} > \text{Br} > \text{I}$. An excess of aromatic compound or solvent i.e. carbon disulphide, CS_2 , dichloromethane, CH_2Cl_2 , n-hexane, nitrobenzene or nitromethane, CH_3NO_2 are used. Olefins and alcohols can also be

employed in place of alkyl halides with protic acids i.e. H_2SO_4 , H_3PO_4 , HF, PPA etc. (Bansal 1978). Several environmental problems were encountered for homogeneous Friedel-Crafts reactions e.g. difficulty in separation and recovery, disposal of used catalyst, corrosion and high toxicity as well as the requirement of stoichiometric amounts of the catalyst. To overcome these problems, considerable efforts have been directed towards the heterogenization of the catalysts particularly for the alkylation reactions of benzene and substituted benzenes.

1.2.3.2 Heterogeneous catalysts

The heterogeneous catalysts are used directly as solid acid catalysts (Sebti *et al.* 2001; Saber *et al.* 2003) or they can be prepared through immobilization of Lewis acids onto different supports i.e. mesoporous molecular sieves, zeolites, clays, alumina, and poly acid salts. Numerous potential advantages are associated with heterogeneous catalysts for Friedel-Crafts reactions especially for the large scale manufacturing industry. These include ease of handling, ease of separation from reaction products, higher thermal stability, possibility of regeneration and decrease in cost due to lower loading of active metal and reusability. Some major disadvantages are also encountered such as availability of different environment of active sites, difficulty associated with the proper characterization of the active sites, blockage of these active sites by in-volatile products and leaching of the active components from the solid support (Masters 1981; Sivasanker 2002).

Lewis acids can be incorporated to the supporting material either directly or via post-synthesis procedures by a multitude of pathways. Accordingly, the properties of the active sites produced are variable and controllable depending on the

synthetic procedure. However, regardless of the synthetic method, the presence of water coordinated to the supported Lewis acid centers will effectively reduce their activity. Therefore, to reach the full potential of these supported Lewis acid catalysts, an efficient drying procedure is required.

The direct method is performed by adding the metal ion salt to the mixture of supporting material precursor before the gelation takes place. However, the metal ion will incorporate to the support network or surface during the gelation process (Tuel 1999). The advantages of this method are the directness, simplicity and the stability of the supported metal species, whereas the random distribution of metal ions is considered the main drawback. In the post synthesis routes, the active metal ions are introduced to a support by either grafting (Choudhary and Mantri 2002) or impregnation methods (Fryxell 2006). The major advantage of this method is that metal ions are more accessible for catalysis but they might be easily leachable. Grafting usually is carried out by slurring the dry support in a pure solvent (e.g. absolute ethanol). The slurred support powder is then grafted with metal species of anhydrous metal salt, usually metal chlorides. After this treatment the sample is washed with the pure solvent and then dried. The impregnation method is done by slurring the dry support powder in the metal salt solution (of appropriate solvent) for a certain time at specific temperature then the solution is evaporated completely.

Despite, the variation in the mode of incorporating the active species (i.e. Lewis acids), good dispersion over the surface of a support is necessary for the production of a homogenous active site environment over the high surface area of the support. For most common supports with surface areas in the range of 100 – 500

$\text{m}^2 \text{g}^{-1}$, a monolayer of a fairly small reagent would correspond to a loading of 1 mmole g^{-1} (Clark 1994).

1.2.4 Types of supporting materials

Mainly, two types of porous materials are used as supports, organic (e.g. polystyrene and resins) or inorganic supports. However, the inorganic supports have been used more frequently. The most commonly used inorganic supports include, mesoporous materials (Sun *et al.* 2006; Vinu *et al.* 2005; Selvaraj and Lee 2006; Okumura *et al.* 2001; Hamdy *et al.* 2005), zeolites e.g. ZSM-5 (Diaz *et al.* 2005), zeolite H β (Choudhary *et al.* 2003), clays (Deshpande *et al.* 2001 and Cseri *et al.* 1995), alumina (Selevati-Niasari *et al.* 2004), poly acids salts (Izumi *et al.* 1995) and carbon nano-tubes and related porous carbons (Pomogailo 1998). The most important factors in determining the best support include surface area of 100 – 1000 $\text{m}^2 \text{g}^{-1}$, pore size (average pore diameter), pore size distribution, total porosity and the acidity (Clark 1994). It is also important to distinguish between crystalline supports with regular pore structure (zeolites), ordered porous materials with a very narrow pore size distribution (mesoporous materials), totally amorphous supports with a wide range of pores and highly irregular surfaces (silica and alumina) and expandable layered structures (clays).

Zeolites which consist of micropores of specific structures may result in molecular shape selectivity. Furthermore, these materials are characterized by high acidity as well as thermal and hydrothermal stability (Corma 1997). But the problem associated with zeolites is the pore size limitation i.e. pores are accessible for smaller molecules only (Corma 1997).

Mesoporous molecular sieves with pores generally arranged in a uniform array are ideal candidates for accommodation of relatively large organic molecules and also they can offer shape selectivity. However, there are numerous disadvantages including the use of hazardous organics as template and the difficulties associated with controlling the conditions during preparation. Amorphous silica with pore diameters up to 10 nm or more doesn't suffer from limitation to accommodate compounds of large molecular sizes but they rarely offer shape selectivity.

The properties of the selected supporting material should be consistent with the requirements of the targeted reaction. Most of the surface area in porous materials is inside those pores (Leofantia *et al.* 1998). The surface –OH groups leads to enormous local surface polarities and help to bind reagent molecules and substrates onto the surface and hence encourage reaction. However, occasionally surface hydroxyl may be highly undesirable particularly for reactions involve hydrophobic reagents (Chiarakorn *et al.* 2007).

Rice husk (RH) as an alternative low cost source of silica was also found to be used as a support in the synthesis of heterogeneous catalysts (Chang *et al.* 2001; Tsay and Chang 2000; Adam *et al.* 2006). Good textural properties of rice husk ash (RHA) silica and metal modified silica are produced by adjusting the preparation conditions. The catalytic activity and stability of RHA (or RHA silica) supported metal catalysts as will be shown latter are comparable to those of other conventional supports. In the following section a brief discussion about RH will be given.

1.3 Rice husk

1.3.1 Composition and production

Rice husks (RH) are the natural sheaths that form on rice grains during their growth and removed as waste during the processing of rice in the mills. The global production of paddy amounted to 600 million tonnes annually giving a total production of 120 million tonnes of RH (Prasetyoko 2006). In Malaysia, it was reported that about 18 million tonnes of paddy were produced annually resulting in about 3.6 million tonnes of RH as waste (Chin *et al.* 2001). Rice husk (RH) has no commercial value, and normally, it will end up going into landfill or burned openly, producing ash of poor quality. Any of these disposal aspects eventually will cause environmental pollution. Currently, this problem has led to many research programs world wide into potential end uses of rice husk.

RH contains low percentages of metallic impurities and considerable amounts of silicon atoms which have been adsorbed from the soil by the rice plant during their growth, the rest of its constituents are organic materials. The actual compositions of RH were found to differ widely and affected by the type of paddy and the soil condition in which it is grown (Mansaray and Ghaly 1999). Furthermore, RH produces about 20 wt. % ash when burned in air. This ash contains >90% silica by mass with minor amounts of metallic elements (Mansaray and Ghaly 1998). Patel *et al.* (1987) reported that the organic materials of RH consist of celluloses (55-60 wt. % including cellulose and hemi cellulose) and lignin (22 wt. %). Mansaray and Ghaly (1998) reported that RH contains cellulose (29.2%), hemicelluloses (20.1%), lignin (20%) and ash (20%). They also calculated the percentages of silica in rice husk ash (RHA) to be in the range 90 – 97 %.

1.3.2 Production of silica from rice husk

Commonly the process of getting pure silica from RH passes through many steps and conditions including pretreatment of raw RH, calcination and extraction of silica from RHA.

The pretreatment processes are followed to remove or minimize all the impurities in the raw RH to insignificant amounts. The adhering soil and some water soluble mineral salts in RH are washed thoroughly with water and distilled water. Most of the metallic impurities are leached out with the aid of mineral acids (i.e. HCl, HNO₃ or H₂SO₄) or a combination of mineral acids before and after the ignition. The acid pretreatment process is applied to decrease the majority of these impurities from RH prior to calcination whereas post-acid washing is followed to remove the small quantities of minerals from RHA.

Liou (2004) reported that, pre-acid leaching of RH significantly reduced the metallic impurities from 4.1 % to around 0.27%. However, omission of acid pretreatment was found to yield silica with a considerably reduced surface area (Conradt *et al.* 1992). Kalapathy *et al.* (2000a) observed that, the initial acid washing of RHA decreased the calcium impurities significantly whereas the water post washing of the xero-gel gave pure silica with total sodium, potassium and calcium contents of < 0.1%. Chakravorty *et al.* (1988) concluded that the pretreatment of RH with dilute HCl, H₂SO₄ or HNO₃ was effective in removing metallic impurities to a substantially lower level. Nevertheless, when the acid concentration was increased the leaching effects were not increased significantly. Furthermore, the leaching capabilities of HCl and HNO₃ were almost similar and they were found to be much